Photochemical & Photobiological Sciences

Accepted Manuscript

This is an *Accepted Manuscript*, which has been through the Royal Society of Chemistry peer review process and has been accepted for publication.

Accepted Manuscripts are published online shortly after acceptance, before technical editing, formatting and proof reading. Using this free service, authors can make their results available to the community, in citable form, before we publish the edited article. We will replace this *Accepted Manuscript* with the edited and formatted *Advance Article* as soon as it is available.

You can find more information about *Accepted Manuscripts* in the Information for Authors.

Please note that technical editing may introduce minor changes to the text and/or graphics, which may alter content. The journal's standard Terms & Conditions and the Ethical guidelines still apply. In no event shall the Royal Society of Chemistry be held responsible for any errors or omissions in this *Accepted Manuscript* or any consequences arising from the use of any information it contains.

ROYAL SOCIETY OF CHEMISTRY

www.rsc.org/pps

Solvent dependent photosensitized singlet oxygen production from an Ir(III) complex: pointing to problems in studies of singlet-oxygen-mediated cell death

Shin-ya Takizawa,[a] Thomas Breitenbach,[b] Michael Westberg,[b] Lotte Holmegaard,[b] Anita Gollmer,[b] Rasmus L. Jensen,[b] Shigeru Murata[a] and Peter R. Ogilby*[b]

[a] Department of Basic Science, Graduate School of Arts and Sciences, The University of Tokyo, Meguro-ku, Tokyo, 153-8902, Japan.

[b] Center for Oxygen Microscopy and Imaging, Department of Chemistry, Aarhus University, Aarhus, 8000 Denmark. E-mail: progilby@chem.au.dk

Abstract

A cationic cyclometallated Ir(III) complex with 1,10-phenanthroline and 2-phenylpyridine ligands photosensitizes the production of singlet oxygen, $O_2(a^1\Delta_g)$, with yields that depend appreciably on the solvent. In water, the quantum yield of photosensitized $O_2(a^1\Delta_g)$ production is small ($\phi_\Delta = 0.036 \pm 0.008$), whereas in less polar solvents, the quantum yield is much larger ($\phi_\Delta = 0.54 \pm 0.05$ in octan-1-ol). A solvent effect on ϕ_Δ of this magnitude is rarely observed and, in this case, is attributed to charge-transfer-mediated processes of non-radiative excited state deactivation that are more pronounced in polar solvents and that kinetically compete with energy transfer to produce $O_2(a^1\Delta_g)$. A key component of this non-radiative deactivation process, electronic-to-vibrational energy transfer, is also manifested in pronounced H_2O/D_2O isotope effects that indicate appreciable coupling between the Ir(III) complex and water. This Ir(III) complex is readily incorporated into HeLa cells and, upon irradiation, is cytotoxic as a consequence of the $O_2(a^1\Delta_g)$ thus produced. The data reported herein point to a pervasive problem in mechanistic studies of photosensitized $O_2(a^1\Delta_g)$-mediated cell death: care must be exercised when interpreting the effective cytotoxicity of $O_2(a^1\Delta_g)$ photosensitizers whose photophysical properties depend strongly on the local environment. Specifically, the photophysics of the sensitizer in bulk solutions may not accurately reflect its intracellular behavior, and the control and quantification of the $O_2(a^1\Delta_g)$ "dose" can be difficult *in vivo*.

Introduction

Singlet oxygen, $O_2(a^1\Delta_g)$, is the lowest excited electronic state of molecular oxygen. It has a unique chemistry that results in the oxygenation of many organic molecules.[1] In this way, $O_2(a^1\Delta_g)$ plays important roles in biology. For example, it is involved in mechanisms of signaling that influence processes ranging from proliferation to death in mammalian cells.[2-7]

$O_2(a^1\Delta_g)$ can be produced in a photosensitized process wherein light is absorbed by a given molecule (the sensitizer) followed by energy transfer from the excited state sensitizer to ground state oxygen, $O_2(X^3\Sigma_g^-)$.[2, 8] The production of $O_2(a^1\Delta_g)$ in this way is used as a clinical tool to destroy/remove cells (*e.g.*, photodynamic cancer treatments,[4, 6]) where the sensitizer is administered as the drug. Although other photo-produced reactive oxygen species, ROS, (*e.g.*, the superoxide ion) can likewise have important biological effects, $O_2(a^1\Delta_g)$ is generally acknowledged as the key cytotoxic agent in photodynamic therapies.[4-6]

The overriding feature in the design and development of an efficient photodynamic drug has long been to prepare photosensitizers with large quantum yields of $O_2(a^1\Delta_g)$ production, ϕ_Δ.[4] Nevertheless, it is recognized that the site of $O_2(a^1\Delta_g)$ production in or near a cell is also an important parameter in influencing the susceptibility of that cell to death.[2, 5, 9-12] Although it is possible to find sensitizers whose ability to make $O_2(a^1\Delta_g)$ varies little with a change in the local environment (*e.g.*, 1-phenalenone),[13-15] this is the exception rather than the rule. Indeed, most sensitizers often show a modest solvent-dependent change in the yield of $O_2(a^1\Delta_g)$ production.[16] This phenomenon has been extensively studied by many practitioners in the field, and it is generally found that an increase in the extent of solvent-controlled charge-transfer (CT) character, either in the sensitizer itself or in the sensitizer-oxygen complex that precedes $O_2(a^1\Delta_g)$ formation, contributes to a low $O_2(a^1\Delta_g)$ yield by facilitating other competitive pathways for excited state

sensitizer deactivation.[8, 17] This is pertinent with respect to the fact that when developing photosensitizers optimized for a specific function (*e.g.*, large two-photon absorption cross section), design parameters that increase CT character are sometimes included.[2] For biological applications, unless steps are taken to control the local environment of such photosensitizers, bulk solution-phase experiments to characterize the photophysics of the sensitizer may not accurately reflect its intracellular behavior (*e.g.*, local solvent effects and non-specific binding to proteins).[18, 19] Specifically, $O_2(a^1\Delta_g)$-mediated cytotoxic effects may derive from only a small population of the sensitizer localized in one intracellular domain, whereas the largest fraction of the intracellular sensitizer localized elsewhere may be benign.

In the present report, we examine a cationic cyclometallated Ir(III) complex with 1,10-phenanthroline (phen) and 2-phenylpyridine (ppy) ligands, denoted $Ir(ppy)_2(phen)^+$ (Fig. 1). We demonstrate that the ability of this compound to sensitize the production of $O_2(a^1\Delta_g)$ depends strongly on the solvent. Moreover, we initially observed that cells incubated in solutions of $Ir(ppy)_2(phen)^+$ were, by far, more sensitive to light than were cells incubated with a typical porphyrin-based sensitizer, for example. This observation might lead one to infer potentially incorrect things about the local intracellular environment of $Ir(ppy)_2(phen)^+$ and/or the effective photo-mediated cytotoxicity of the compound. On the basis of these points, we set out to more fully elucidate the photo-initiated properties of $Ir(ppy)_2(phen)^+$, including its behavior when incorporated in a cell. The results we obtain address a pervasive problem and should thus be useful in attempts to characterize photosensitizers that can better contribute to understanding mechanisms of $O_2(a^1\Delta_g)$-mediated cell signaling and cell death.

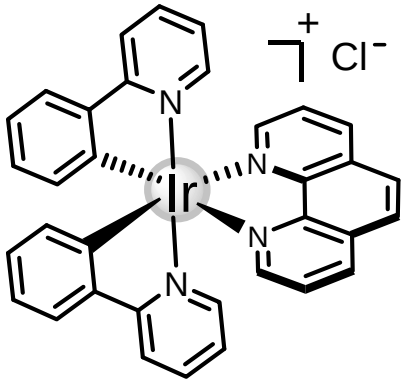

Fig. 1. Structure of the bis(2-phenylpyridine)-1,10-phenanthroline-ligated Ir(III) complex, denoted $Ir(ppy)_2(phen)^+$, used as the $O_2(a^1\Delta_g)$ sensitizer in this study.

Experimental

Instrumentation and approach. Published articles describe (1) the systems and approaches used to obtain $O_2(a^1\Delta_g)$ quantum yields, excited state lifetimes, and two-photon absorption cross sections,[20-24] and (2) the microscopes and techniques used to both perturb and image cells.[11, 25, 26] Lifetimes and quantum yields of the $Ir(ppy)_2(phen)^+$ phosphorescent state were independently determined using Hamamatsu Photonics Quantaurus Tau and QY spectrometers, respectively. Note that the use of this QY spectrometer to determine phosphorescence quantum yields does not require the use of an emission standard.

Quantum yields of $Ir(ppy)_2(phen)^+$-sensitized $O_2(a^1\Delta_g)$ production were determined by recording the integrated intensity of the time-resolved $O_2(a^1\Delta_g) \rightarrow O_2(X^3\Sigma_g^-)$ phosphorescence signal at 1275 nm and comparing it to the integrated intensity of the $O_2(a^1\Delta_g) \rightarrow O_2(X^3\Sigma_g^-)$ phosphorescence signal obtained from a reference standard. Because experiments were performed in water, CH_2Cl_2 and octan-1-ol, we opted to use standards dissolved in these particular solvents to avoid (1) optical detection problems that might derive from changes in the solvent refractive index,[27] and (2) problems that might arise as a consequence of solvent-dependent changes in the

rate constant for $O_2(a^1\Delta_g)$ radiative deactivation.[8, 28] The standards used were the 2-sulfonic acid derivative of phenalenone in water ($\phi_\Delta = 0.97 \pm 0.06$),[15] phenalenone in CH_2Cl_2 ($\phi_\Delta = 0.96 \pm 0.08$),[15] and phenalenone in octan-1-ol ($\phi_\Delta = 0.96 \pm 0.08$). For our standard in octan-1-ol, we relied on the fact that the available experimental evidence indicates that the yield of $O_2(a^1\Delta_g)$ sensitized by 1-phenalenone varies little with a change in solvent.[13-15] Thus, we assumed that the ϕ_Δ value for $O_2(a^1\Delta_g)$ production in octan-1-ol would be the same as that in CH_2Cl_2. Two-photon absorption cross section measurements were performed using fluorescein in alkaline H_2O as the fluorescent standard ($\delta_{800\ nm} = 36 \pm 5$ GM).[29, 30]

For the two-photon initiated cell kill experiments, the 800 nm (spectral fwhm ~ 12 nm) output of a fs laser operating at 80 MHz (Mai Tai from Spectra Physics) was coupled onto a microscope objective (60× Olympus LUMPlanFI/IR, water immersion, NA 0.9) in an inverted microscope (Olympus IX71).[11, 12, 25, 31] The optics used result in a beam diameter at the focused waist of ~ 1 μm.[31] However, given that the probability of the two-photon transition depends on the square of the incident light intensity, only the light in a smaller spatial domain at the center of the focus results in the creation of excited states.[31] For all experiments, the average laser power delivered to the cells at the microscope stage was 2.4 mW. With a focused beam diameter of ~ 1 μm, this corresponds to ~ 3×10^5 W/cm^2. However, the comparatively small two-photon absorption cross sections of the dyes used ensure that only a small fraction of this incident light is actually absorbed.[12]

Chemicals. $Ir(ppy)_2(phen)^+$ [32] and the 2-sulfonic acid derivative of phenalenone[33] were synthesized as described in the references cited. D_2O (99% D) was obtained from EurisoTop or Acros Organics, and ER-Tracker was obtained from Invitrogen/Molecular Probes. All other chemicals were obtained from Sigma-Aldrich, Acros Organics, or Wako Pure Chemical Industries,

Ltd. and used as received. De-oxygenated solutions were obtained by gentle bubbling with argon for 20 min prior to a given measurement.

Cells. The general methods used to prepare and handle HeLa cells, and to add fluorescent markers to these cells, have been published.[10-12, 25, 34]

$Ir(ppy)_2(phen)^+$ was incorporated into the cells using the following procedure: (1) The growth medium was removed and the cells were washed twice with our so-called artificial bath medium, ABM, which is composed of 140 mM NaCl, 3.5 mM KCl, 2 mM $CaCl_2$, 2 mM $MgCl_2$, 1.25 mM NaH_2PO_4, 10 mM D-(+)-glucose and 10 mM HEPES, all of which is maintained at pH 7.4. (2) The cells were then incubated with an ABM solution of $Ir(ppy)_2(phen)^+$ at a specified concentration in the range 0.1 – 20 μmole L^{-1} for 15 min. ABM was used because $Ir(ppy)_2(phen)^+$ has a high affinity for the proteins that are present in the normal growth medium. (3) The $Ir(ppy)_2(phen)^+$ solution was then removed and the cells washed twice with $Ir(ppy)_2(phen)^+$-free ABM. (4) The cells were placed into glass bottom coverslips (LabTek, Th. Geyer) and kept under either ABM for the short-term microscope-based experiments (< 6 h) or growth medium for longer-term experiments (> 6 h).

Upon exposure of a given cell population to ABM containing $Ir(ppy)_2(phen)^+$, we quantified the amount of $Ir(ppy)_2(phen)^+$ incorporated into the cells using the following procedure:[35] (1) After exposure of the cells to $Ir(ppy)_2(phen)^+$ for 15 min, we washed the cells twice with $Ir(ppy)_2(phen)^+$-free ABM, (2) we lysed the cells using 400 μL DMSO, then (3) we centrifuged the mixture and recorded absorption and emission spectra of the supernatant liquid. The resultant spectra were calibrated against spectra of $Ir(ppy)_2(phen)^+$ standard solutions, and the concentrations thus obtained were then normalized by the number of cells in that particular sample to yield an average amount of $Ir(ppy)_2(phen)^+$ per cell.

ER-Tracker was incorporated into the cells by first removing the growth medium and washing the cells twice with ABM. The cells were then incubated with an ABM solution of 1 μM ER-Tracker for 30 min. Thereafter, the cells were washed twice with ABM.

Results and discussion

1. Characterizing $Ir(ppy)_2(phen)^+$ photophysics in bulk solutions

Absorption and emission spectra of $Ir(ppy)_2(phen)^+$ in a number of solvents are shown in Fig. 2. A red shift in the emission spectrum as the polarity of the solvent is increased, and as seen in our data, is often described as reflecting CT character in the emitting state.[32, 36, 37] We return to this point below.

Other photophysical parameters of $Ir(ppy)_2(phen)^+$ pertinent to the present study were determined using established procedures and are shown in Table 1 and discussed in separate sections below.

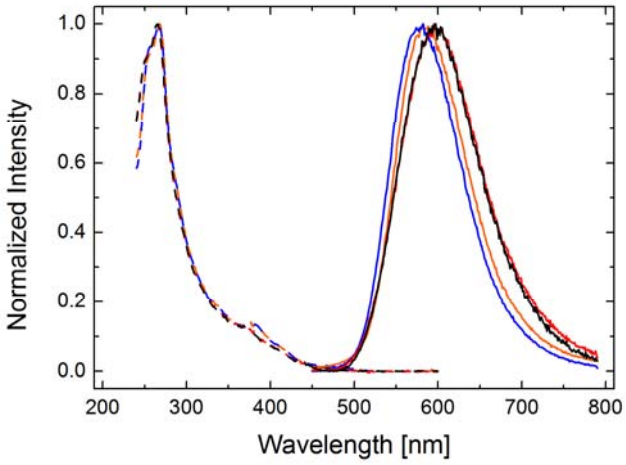

Fig. 2. Normalized absorption (dashed lines) and emission (solid lines) spectra of $Ir(ppy)_2(phen)^+$ in H_2O (black), D_2O (red), octan-1-ol (orange) and CH_2Cl_2 (blue). When we expand the intensity scale of our absorption spectra in the range ~ 450-500 nm we observe a weak band that has been previously observed[32] and assigned to the population of the lowest triplet state of $Ir(ppy)_2(phen)^+$.

Table 1. Selected Photophysical Parameters of $Ir(ppy)_2(phen)^+$ determined in four solvents.[a]

Solvent	ϕ_Δ	f_P[b]	ϕ_{nr}^{air}	ϕ_P^{air}	ϕ_P^{Ar}	τ_P^{air} (ns)	τ_P^{Ar} (ns)
H_2O	0.036 ± 0.008	0.11 ± 0.01	0.85 ± 0.04	0.042 ± 0.001	0.051 ± 0.004	92 ± 4	103 ± 2
D_2O	0.064 ± 0.006	0.23 ± 0.02	0.68 ± 0.03	0.086 ± 0.003	0.12 ± 0.01	212 ± 8	276 ± 8
CH_2Cl_2	0.53 ± 0.04	0.77 ± 0.09	0.14 ± 0.01	0.095 ± 0.004	0.42 ± 0.02	176 ± 10	761 ± 35
Octan-1-ol	0.54 ± 0.05	0.75 ± 0.01	0.13 ± 0.01	0.12 ± 0.01	0.45 ± 0.02	208 ± 1	842 ± 11

a) Determined under air-saturated and de-oxygenated conditions. The latter was achieved by bubbling with solvent-saturated Ar gas for 20 min prior to a measurement.

b) Fraction of the $Ir(ppy)_2(phen)^+$ phosphorescent state that is quenched by oxygen under air-saturated conditions. This number was obtained through the expression $1 - (\tau_P^{air}/\tau_P^{Ar})$.

Quantum yields of $Ir(ppy)_2(phen)^+$ phosphorescence. Phosphorescence quantum yields, ϕ_p, and lifetimes of the $Ir(ppy)_2(phen)^+$ phosphorescent state, τ_p, were determined in both air-saturated and de-oxygenated solutions (Table 1). The data recorded in water show an appreciable isotope effect that is consistent with D_2O/H_2O solvent effects recorded from related metal complexes.[38-42] These data indicate that coupling between the chromophore and the surrounding water molecules is sufficiently strong and that energy transfer to solvent vibrational modes is important in the non-radiative deactivation of the $Ir(ppy)_2(phen)^+$ excited electronic state. The lower O-D vibrational frequency results in a smaller rate constant for non-radiative deactivation and this, in turn, results in a larger quantum yield for radiative deactivation. For example, if we assume that the rate constant for $Ir(ppy)_2(phen)^+$ radiative deactivation, k_r, does not change appreciably upon H/D isotopic substitution in water, then we can use experimental data on τ_p in H_2O and D_2O and ϕ_p in H_2O to calculate ϕ_p in D_2O (eqn (1)).

$$\frac{k_r^{D2O}\tau_p^{D2O}}{k_r^{H2O}\tau_p^{H2O}}\,\phi_p^{H2O} = \phi_p^{D2O} \qquad (1)$$

The numbers obtained through this exercise are consistent with the experimentally determined ϕ_p values in D_2O (Table 1). [*i.e.*, ϕ_p^{Ar}(calc) = 0.14 ± 0.02; ϕ_p^{Ar}(expt) = 0.12 ± 0.01 and ϕ_p^{air}(calc) = 0.097 ± 0.010; ϕ_p^{air}(expt) = 0.086 ± 0.003]

Although the discussion below focuses on solvent-dependent CT effects, the preceding interpretation of the D_2O/H_2O solvent effect means that we cannot exclude the possibility that, to some extent, the data recorded in octan-1-ol and CH_2Cl_2 also reflect (1) a comparatively poor coupling between $Ir(ppy)_2(phen)^+$ and these solvents and (2) the comparative lack of vibrational modes in these solvents that can act as a sink for the excitation energy of $Ir(ppy)_2(phen)^+$.

Quantum yield of $O_2(a^1\Delta_g)$ production. Quantum yields of $Ir(ppy)_2(phen)^+$-sensitized $O_2(a^1\Delta_g)$ production were determined in air-saturated solutions (Table 1). Values of ϕ_Δ thus obtained can therefore be compared to the values of ϕ_p that were likewise obtained from air-saturated solutions.

The data obtained indicate that $Ir(ppy)_2(phen)^+$ is a very inefficient source of $O_2(a^1\Delta_g)$ when dissolved in water (*e.g.*, ϕ_Δ = 0.036 ± 0.008 in H_2O). In contrast, we ascertained that the $Ir(ppy)_2(phen)^+$-sensitized yield of $O_2(a^1\Delta_g)$ is 0.54 ± 0.05 in octan-1-ol and 0.53 ± 0.04 in CH_2Cl_2. It is clear that the ϕ_Δ values obtained in these less polar solvents ($\varepsilon_{dichloromethane}$ = 8.9 and $\varepsilon_{octanol}$ = 10.3) are appreciably larger than that seen in water (ε ~ 80).

In all of our ϕ_Δ experiments, we found no evidence that $Ir(ppy)_2(phen)^+$ quenches $O_2(a^1\Delta_g)$ under our conditions. Specifically, the lifetime of $O_2(a^1\Delta_g)$ observed in the D_2O experiments was 67 ± 1 μs, whereas it was 95 ± 1 μs in CH_2Cl_2. These numbers are consistent with what is expected for $O_2(a^1\Delta_g)$ deactivation mediated solely by the solvent.[43] This observation is likewise consistent with what has been reported in related studies of Ir(III) compounds.[44, 45]

It is relevant to note one feature about the CH_2Cl_2 data. A larger ϕ_Δ value of 0.93 has been determined for the $Ir(ppy)_2(phen)^+$-sensitized production of $O_2(a^1\Delta_g)$ in a CH_2Cl_2-CH_3OH (9:1) mixture using an indirect method in which $O_2(a^1\Delta_g)$ was trapped in a chemical reaction.[44] Although there are disadvantages to quantifying ϕ_Δ values using a chemical trap as opposed to the direct detection of $O_2(a^1\Delta_g)$ phosphorescence,[16] this value of 0.93 likely differs from the value of 0.53 shown in Table 1 principally as a consequence of the fact that these earlier experiments were performed in an oxygen-saturated solvent where a larger fraction of the $Ir(ppy)_2(phen)^+$ excited states are quenched by $O_2(X^3\Sigma_g^-)$ (note that f_P in our air-saturated CH_2Cl_2 experiments is only 0.77 ± 0.09, Table 1).

We take this opportunity to also comment on another aspect of photosensitized $O_2(a^1\Delta_g)$ experiments performed in CH_2Cl_2 solutions. One molecule commonly added as a stabilizer to commercial CH_2Cl_2 is amylene. Upon 400 nm irradiation of CH_2Cl_2 that contains amylene, we are able to detect a $O_2(a^1\Delta_g)$ phosphorescence signal. Although CH_2Cl_2 does not absorb at 400 nm, amylene or its polymerized products do absorb light at this wavelength and can sensitize the production of $O_2(a^1\Delta_g)$ which, in turn, can yield a larger and erroneous value of ϕ_Δ for a given sensitizer dissolved in CH_2Cl_2. To avoid the necessity of accounting for this amylene-sensitized signal, it is advisable to use CH_2Cl_2 stabilized with methanol instead.

Characterizing the $O_2(a^1\Delta_g)$ precursor. Over the years, an appreciable effort has been expended to quantify the photophysical properties of cyclometallated Ir(III) complexes,[46, 47] including the effectiveness of these complexes to act as $O_2(a^1\Delta_g)$ photosensitizers.[44, 45, 48-50] The evidence provided indicates that Ir(III) complexes are generally quite luminescent and also sensitize the production of $O_2(a^1\Delta_g)$ in high yield (*i.e.*, ϕ_Δ values in the range 0.5-1.0). However, most of the pertinent measurements to this end were made in non-polar solvents (*e.g.*, benzene) that would not

promote a comparatively large amount of CT character in the system. With respect to our present study, correspondingly small values of ϕ_Δ have nevertheless also been observed from cyclometallated complexes, including examples with Os(II) complexes ($\phi_\Delta = 0.05 \pm 0.01$ in CH_3CN)[51] and Ru(II) complexes ($\phi_\Delta \sim 0.04 - 0.25$ in D_2O).[42] Reasonable explanations for the large variation in photophysical properties of these compounds can be found in the effects that the cyclometallating ligands and solvent have on the relative energetics of the excited states and the extent to which metal-to-ligand charge-transfer (MLCT) states play a role in characterizing the photoinitiated behavior.[32, 37, 42, 45, 46, 51, 52]

With these earlier studies in mind, the small values of ϕ_Δ and ϕ_p obtained for $Ir(ppy)_2(phen)^+$ in D_2O and H_2O are consistent with a model in which unimolecular non-radiative deactivation of the $Ir(ppy)_2(phen)^+$ phosphorescent state, that also serves as the $O_2(a^1\Delta_g)$ precursor, is more efficient than the bimolecular process in which that state is quenched by $O_2(X^3\Sigma_g^-)$. Indeed, the lifetime of the $Ir(ppy)_2(phen)^+$ phosphorescent state in a de-oxygenated H_2O solution (103 ± 2 ns) is not appreciably longer than that in an air-saturated solution (92 ± 4 ns) indicating that only 11 % of the $Ir(ppy)_2(phen)^+$ phosphorescent states are quenched by $O_2(X^3\Sigma_g^-)$ under these conditions (Table 1). Our data also allow us to make a statement about those $Ir(ppy)_2(phen)^+$ phosphorescent states that are quenched by $O_2(X^3\Sigma_g^-)$. Specifically, within the excited-state $Ir(ppy)_2(phen)^+$-$O_2(X^3\Sigma_g^-)$ encounter complex, it appears that CT-mediated deactivation processes likewise effectively compete with energy transfer to make $O_2(a^1\Delta_g)$ (*e.g.*, $f_p >> \phi_\Delta$ in water). The latter is an established phenomenon.[8, 17, 42, 45]

In contrast, in the solvents with a much smaller dielectric constant (*i.e.*, CH_2Cl_2 and octan-1-ol), the extent to which the excited state processes involve CT character decreases. In turn, bimolecular quenching of the $Ir(ppy)_2(phen)^+$ phosphorescent state by $O_2(X^3\Sigma_g^-)$ becomes kinetically competitive; $\sim 75\%$ of the $Ir(ppy)_2(phen)^+$ triplet states are quenched by $O_2(X^3\Sigma_g^-)$ in

air-saturated solutions (Table 1). Moreover, in these solvents, the inequality $f_p > \phi_\Delta$ is not as great as in water.

To better represent the preceding points, we used the relationship of $1 - f_P - \phi_p^{air}$ to yield values for the quantum yield of unimolecular non-radiative $Ir(ppy)_2(phen)^+$ deactivation, ϕ_{nr}, in these four solvents (Table 1).

Two-photon absorption cross sections. We also quantified the two-photon absorption cross sections, δ, of $Ir(ppy)_2(phen)^+$ in these same four solvents. Data were obtained by comparing the probability of a two-photon initiated process in $Ir(ppy)_2(phen)^+$ to the probability of a two-photon initiated process in a standard molecule for which δ is known. For the present experiments, the intensity of two-photon initiated $Ir(ppy)_2(phen)^+$ phosphorescence was compared to the intensity of two-photon initiated fluorescence from fluorescein in alkaline H_2O. Using a fs-laser-based approach outlined in previous publications,[20, 21, 24] measurements were made with excitation at 800 nm. The data obtained yielded $Ir(ppy)_2(phen)^+$ absorption cross sections that were, within the margins of our errors, independent of the solvent used: $\delta_{800} = 1.9 \pm 0.5$ GM in H_2O, $\delta_{800} = 2.1 \pm 0.5$ GM in D_2O, $\delta_{800} = 2.8 \pm 0.7$ GM in octan-1-ol, and $\delta_{800} = 2.4 \pm 0.6$ GM in CH_2Cl_2 (1 GM = 10^{-50} cm^4 s $photon^{-1}$). Although these absorption cross sections are ~ 10 times smaller than cross sections that have previously been reported for similar Ir(III) complexes,[53, 54] it is important to note that we did not record the full two-photon spectrum and, as such, may not be recording data at the absorption band maximum. Nevertheless, for the purpose of our present study, and as outlined below, we do not expect an appreciable solvent-dependent shift in the two-photon spectrum. As such, when compared to each other, these values of δ_{800} provide useful insight.

It is acknowledged that an increased amount of CT character in one of the states involved in the two-photon process can result in a larger absorption cross section.[55] Thus, at first glance, the

solvent-independent values of δ shown above may seem anomalous, certainly in light of our CT-based interpretation of the data shown in Table 1. However, the one-photon data shown in Fig. 2 provide what is perhaps the clearest way to explain these observations and justify our CT-based perspective. The states involved in $Ir(ppy)_2(phen)^+$ light absorption do not appear to be influenced by an appreciable amount of CT character; the one-photon absorption spectrum is essentially independent of solvent. On the other hand, the $Ir(ppy)_2(phen)^+$ state from which light is emitted, and that is the precursor to $O_2(a^1\Delta_g)$ production, responds to solvent in a way that indicates it has a comparatively greater amount of CT character.

2. $Ir(ppy)_2(phen)^+$-sensitized $O_2(a^1\Delta_g)$-mediated cell death

One observation that prompted this study was that, under our normal preparative conditions, cells incubated in media containing $Ir(ppy)_2(phen)^+$ were very sensitive to ambient laboratory lighting (*i.e.*, typical fluorescent lights). We found this surprising since the one-photon absorption spectrum of $Ir(ppy)_2(phen)^+$ has only a weak tail that extends out to wavelengths longer than 400 nm (Fig. 2; the extinction coefficient at 420 nm is 3110 M^{-1} cm^{-1} in octan-1-ol). On the other hand, and again under our normal preparative conditions, cells containing typical porphyrin-based $O_2(a^1\Delta_g)$ sensitizers generally tolerate a small amount of ambient lighting, despite the fact that the strongly absorbing Soret band at ~ 420 nm overlaps well with the first intense emission band of a typical fluorescent room light. Thus, we wanted to put this apparent photo-induced "super-cytotoxicity" of $Ir(ppy)_2(phen)^+$ on a more quantitative footing.

2.a. Incorporation of $Ir(ppy)_2(phen)^+$ in mammalian cells

Solubility of $Ir(ppy)_2(phen)^+$. Although the octanol/water partition coefficient for $Ir(ppy)_2(phen)^+$ is not large ($\log P_{o/w} = 1.67$),[56] it nevertheless indicates that an appreciable fraction of the molecules

preferentially localize in octanol instead of water. This clearly has ramifications in the intracellular localization of $Ir(ppy)_2(phen)^+$ and in the solvent-dependent photophysics of $Ir(ppy)_2(phen)^+$ pertinent to $O_2(a^1\Delta_g)$ production.

Quantifying $Ir(ppy)_2(phen)^+$ incorporation. There appears to be a general consensus in the literature that cellular uptake of Ir(III) complexes is most efficient for lipophilic compounds.[57] Our data are consistent with this expectation. Upon exposure of a given cell population to ABM containing $Ir(ppy)_2(phen)^+$, we quantified the amount of $Ir(ppy)_2(phen)^+$ incorporated into the cells using the procedure described in the Experimental Section. The pertinent data are shown in Figure 3. These data show that the amount of $Ir(ppy)_2(phen)^+$ in a cell scales according to the amount of $Ir(ppy)_2(phen)^+$ in the extracellular medium when the latter is in the concentration range of 10^{-7} to 10^{-5} M.

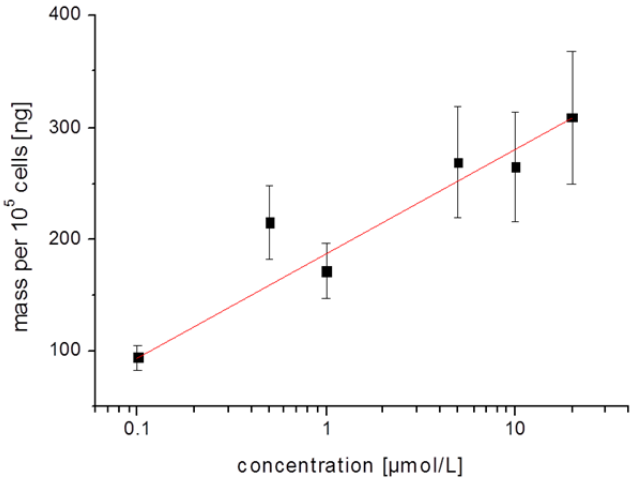

Fig. 3. Semi-logarithmic plot of the amount of $Ir(ppy)_2(phen)^+$ incorporated in a cell against the concentration of $Ir(ppy)_2(phen)^+$ added to the extracellular medium. The solid line is a linear fit to the data and is meant simply as a guide for the eye.

Intracellular localization of $Ir(ppy)_2(phen)^+$. An image of HeLa cells based on the emission from $Ir(ppy)_2(phen)^+$ suggests that, upon exposing HeLa cells to a medium containing $Ir(ppy)_2(phen)^+$,

$Ir(ppy)_2(phen)^+$ is preferentially incorporated in certain organelles (Fig. 4a). Based on independent images of organelle-localized dyes,[58, 59] we infer from Fig. 4a that $Ir(ppy)_2(phen)^+$ preferentially localizes in the mitochondria. This is a reasonable assignment given the predilection for the localization of positively charged compounds in the mitochondrial membrane.[60] Unfortunately, attempts to be more specific in this regard were somewhat complicated. For example, rhodamine 123 (Rh123) localizes in the mitochondria and yields distinct fluorescence images that show the typical mitochondrial association with cytoskeletal proteins (Fig. 4b). However, in an attempt to perform a standard emission-based co-localization study, addition of $Ir(ppy)_2(phen)^+$ to cells that contain Rh123 caused a pronounced blurring of both the Rh123 image (Fig. 4c) and the $Ir(ppy)_2(phen)^+$ image (Fig. 4d). In itself, this suggests that $Ir(ppy)_2(phen)^+$ is indeed localized in the mitochondria; $Ir(ppy)_2(phen)^+$ either displaces the mitochondrial-localized Rh123 or, when combined with Rh123, sufficiently perturbs the mitochondria such that both Rh123 and $Ir(ppy)_2(phen)^+$ are no longer specifically localized. It is important to note, however, that cells containing both $Ir(ppy)_2(phen)^+$ and Rh123 do not show morphological signs of apoptosis or necrosis over a 2 h period and thus, by inference, mitochondrial function has not been adversely perturbed.

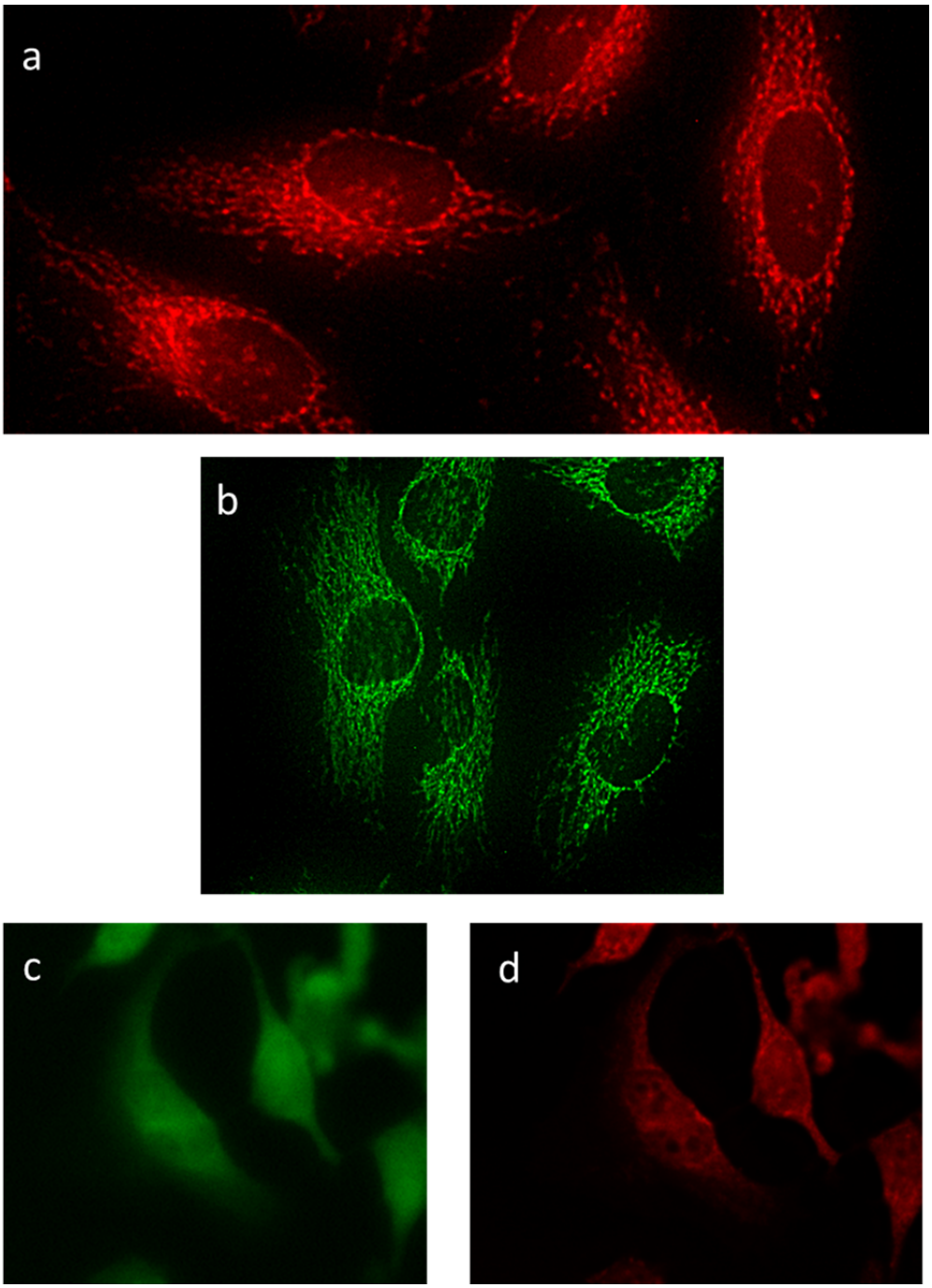

Fig. 4. (a) Image of HeLa cells based on the emission of $Ir(ppy)_2(phen)^+$. These cells were incubated in a medium containing 10 μM $Ir(ppy)_2(phen)^+$ for 15 min. (b) Image of HeLa cells based on the fluorescence of Rh123 under $Ir(ppy)_2(phen)^+$-free conditions. (c and d) Images of HeLa cells into which Rh123 was first incorporated and then $Ir(ppy)_2(phen)^+$ was added to the medium. Panel c shows the Rh123 image and panel d the corresponding image based on $Ir(ppy)_2(phen)^+$ emission. The colors used in the images were arbitrarily chosen. $Ir(ppy)_2(phen)^+$ was excited at 420 nm and Rh123 at 480 nm, which allows us to discriminate between these respective dyes.

On the basis of other images of organelle-localized dyes,[58, 59] Fig. 4a could also be interpreted to indicate that $Ir(ppy)_2(phen)^+$ localizes in the endoplasmic reticulum, ER. This perspective is reinforced by the image of HeLa cells shown in Fig. 5a which is based on the fluorescence of a dye that preferentially localizes in the ER (the so-called "ER Tracker") and which appears very similar to the $Ir(ppy)_2(phen)^+$ image in Fig. 4a. Upon incorporating $Ir(ppy)_2(phen)^+$ into cells that already contain ER-Tracker, the ER-Tracker-based fluorescence images change slightly suggesting a possible $Ir(ppy)_2(phen)^+$-induced morphological change in the cell and/or a $Ir(ppy)_2(phen)^+$-induced relocalization of ER-Tracker (Fig. 5b). However, the $Ir(ppy)_2(phen)^+$-dependent changes observed are clearly not as pronounced as those observed with Rh123 (Fig. 4c). Images of the cells based on the combined emission of $Ir(ppy)_2(phen)^+$ and the ER-Tracker indicate that, when in the cell together, these dyes do not localize in the same intracellular domain (Fig. 5c).

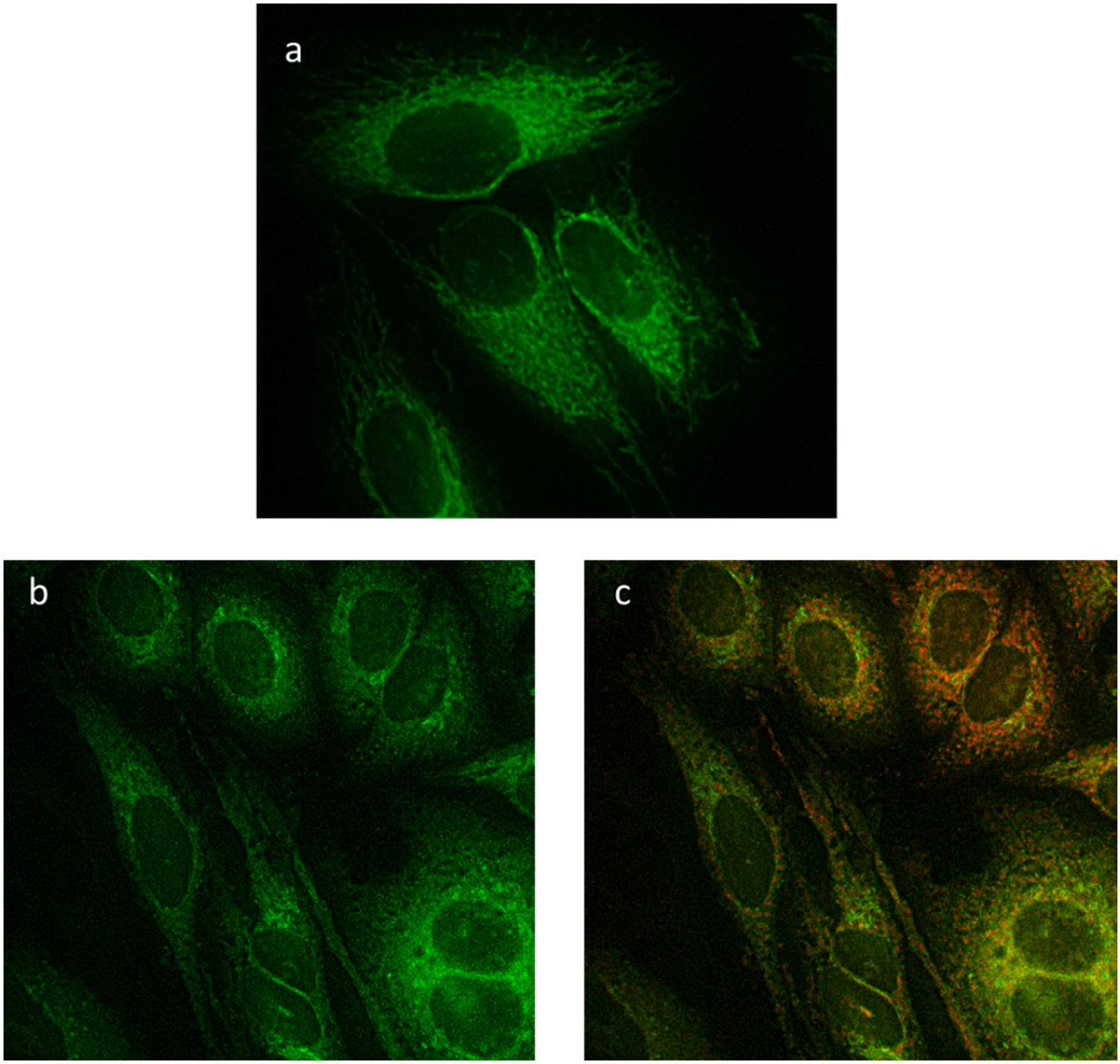

Fig. 5. (a) Image of HeLa cells based on the fluorescence of ER-Tracker. (b) Image of HeLa cells based on the fluorescence of ER-Tracker after the addition of $Ir(ppy)_2(phen)^+$ to the extracellular medium. (c) ER-Tracker-based image of the cells shown in panel b that also includes emission data from the $Ir(ppy)_2(phen)^+$ incorporated into the cells (the color red was used for the latter). The Pearson co-localization coefficient obtained from this image is 0.28 indicating that the ER-Tracker and $Ir(ppy)_2(phen)^+$ are not localized in the same place. $Ir(ppy)_2(phen)^+$ was excited at 420 nm and ER-Tracker at 480 nm, which allows us to discriminate between these respective dyes. The colors used in the images were arbitrarily chosen.

The emission spectrum recorded from a cell containing $Ir(ppy)_2(phen)^+$ (Fig. 6) indicates that $Ir(ppy)_2(phen)^+$ is localized in lipophilic domains in the cell (*e.g.*, a membrane).

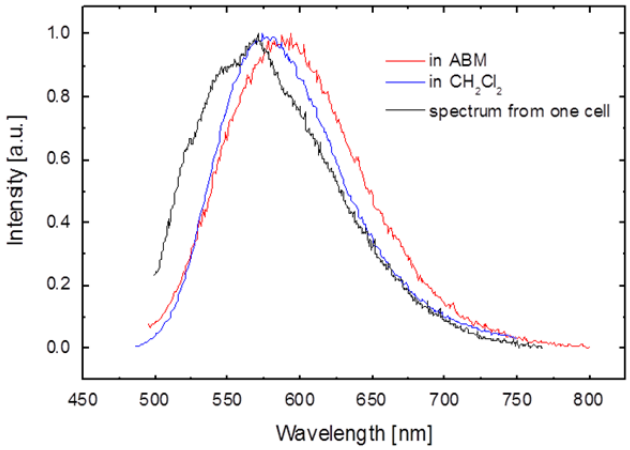

Fig. 6. Emission spectra recorded from $Ir(ppy)_2(phen)^+$-containing systems upon excitation at 420 nm. The spectrum recorded from a single cell is more consistent with that recorded from a lipophilic solvent rather than a hydrophilic solvent.

On the basis of the preceding information, particularly the data in Fig. 4, we conclude that $Ir(ppy)_2(phen)^+$ is indeed most likely localized in the mitochondria. Further confirmation for this assignment is provided in the next section. This assignment is also consistent with our initial observation that cells containing $Ir(ppy)_2(phen)^+$ are uniquely sensitive to light, given the current understanding that the production of $O_2(a^1\Delta_g)$ in the mitochondria is more deleterious to the cell than the production of $O_2(a^1\Delta_g)$ in other organelles.[5, 9, 61]

2.b. Controlling, characterizing and quantifying $Ir(ppy)_2(phen)^+$-sensitized cell death

Incorporation of a reference sensitizer in a cell. To help quantify the photo-induced cytotoxicity of $Ir(ppy)_2(phen)^+$, we opted to use protoporphyrin IX (PpIX) as a reference sensitizer. Within the context of the present study, one important aspect of PpIX is that it is also readily localized inside

the mitochondria. Specifically, PpIX can be generated endogenously by incubating the cells with 5-aminolevulininc acid (ALA) which is a biosynthetic precursor of PpIX.[62] The final steps in the conversion of ALA into PpIX occur in the mitochondria and, as such, PpIX is initially localized in this organelle.[26, 62]

Although PpIX is routinely used as an effective photodynamic agent,[4, 12] to our knowledge there has only been one published study of its efficiency as a $O_2(a^1\Delta_g)$ sensitizer; a ϕ_Δ value of 0.56 ± 0.03 was determined in a study in which the extent of lysozyme deactivation upon PpIX irradiation was used to quantify ϕ_Δ.[63] However, this number is consistent with the large amount of ϕ_Δ data reported for the dimethyl ester of PpIX,[64] confirming that PpIX is indeed a reasonable choice as a reference standard for $O_2(a^1\Delta_g)$ production for our current experiments.

In previous studies, we used the intensity of PpIX fluorescence from a given cell to assess the relative number of PpIX excited states produced upon irradiation.[12] Although there are errors associated with this approach, including errors associated with values of the quantum yield of PpIX emission that depend on the local environment,[65] the data thus obtained nevertheless yield a useful parameter which, along with the quantum yield of PpIX-sensitized $O_2(a^1\Delta_g)$ production, allows us to quantify the photo-produced dose of $O_2(a^1\Delta_g)$ in that cell.[12] As outlined below, we used the same approach to control and quantify $Ir(ppy)_2(phen)^+$-sensitized $O_2(a^1\Delta_g)$ production in a cell.

PpIX and $Ir(ppy)_2(phen)^+$ co-localization study. An emission-based co-localization study shows that $Ir(ppy)_2(phen)^+$ is localized very close to the ALA-produced PpIX (Fig.7). This study also shows that, like the case of Rh123 and $Ir(ppy)_2(phen)^+$ discussed above, the presence of PpIX and $Ir(ppy)_2(phen)^+$ together in a cell appears to result in the general blurring of what is usually a clear image of mitochondria associated with skeletal proteins (see Fig. 4a for the pertinent

$Ir(ppy)_2(phen)^+$-based image and Breitenbach, *et al*.[26] for the PpIX-based image). We take this information as further confirmatory evidence that $Ir(ppy)_2(phen)^+$ is localized in the mitochondria.

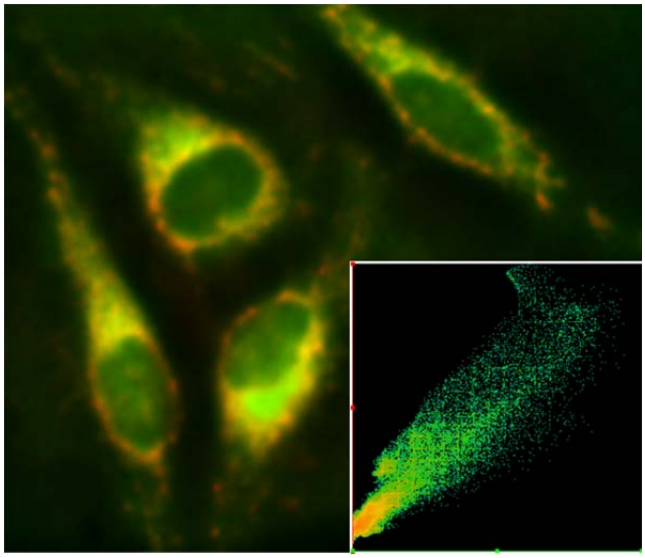

Fig. 7. Image of HeLa cells based on the emission from $Ir(ppy)_2(phen)^+$ (green) and PpIX (red). Co-localization yields the orange color. Cells were first incubated for 4 h in a medium containing 1 mM ALA to produce intracellular mitochondrial-localized PpIX. Thereafter, the cells were incubated for 15 min in a medium containing 10 μM $Ir(ppy)_2(phen)^+$. **(Inset)** Two-dimensional co-localization diagram that yields a Pearson coefficient of 0.91 indicating that, in places where PpIX is localized, $Ir(ppy)_2(phen)^+$ is very nearby. The plot also shows that, for cells which also contain PpIX, $Ir(ppy)_2(phen)^+$ de-localizes into a larger area of the cytoplasm.

As we have indicated, PpIX produced endogenously from ALA is initially localized inside the mitochondria. The $Ir(ppy)_2(phen)^+$-induced blurring of the PpIX image (Fig. 7) confirms that, when using PpIX as a reference $O_2(a^1\Delta_g)$ sensitizer in a cell kill study, $Ir(ppy)_2(phen)^+$ cannot be in that same cell, and *vice versa*. Thus, the cell kill experiments described below were performed using cells that contained only PpIX and, independently, only $Ir(ppy)_2(phen)^+$.

Two-photon irradiation of intracellular sensitizers. Over the years, sensitizer excitation and $O_2(a^1\Delta_g)$ production in cells have traditionally been achieved in a one-photon process wherein the energy of an incident photon is resonant with a transition in the sensitizer. However, sensitized $O_2(a^1\Delta_g)$ production can also occur via the simultaneous absorption of two low-energy photons that, by themselves, are not resonant with a transition in the sensitizer.[2] Although the transition probabilities for this latter process are smaller and larger photon fluxes are generally required, it nevertheless has distinct mechanistic advantages with respect to spatial and spectral control of the excited states produced in a cell.[2, 7, 11, 12, 25, 66] As such, we performed the present study using spatially-localized two-photon excitation of intracellular PpIX and, independently, $Ir(ppy)_2(phen)^+$ at 800 nm. Although two-photon absorption cross sections have been determined for both PpIX and $Ir(ppy)_2(phen)^+$ at this wavelength, it is not necessary to use these parameters when controlling the dose of sensitized $O_2(a^1\Delta_g)$ production. Rather, as outlined in the next section, it is sufficient to monitor the relative intensities of emission from these molecules as a measure of the number of excited states produced.

Controlling the $O_2(a^1\Delta_g)$ dose. To properly assess the photo-initiated cytotoxic effects of $Ir(ppy)_2(phen)^+$ relative to PpIX, we need to ensure that comparable amounts of $O_2(a^1\Delta_g)$ are produced in these respective experiments. This can be achieved by adjusting either (a) the actinic laser power, and/or (b) the intracellular sensitizer concentration using the emission intensity of PpIX and, independently, $Ir(ppy)_2(phen)^+$ from the cells as dosimetric parameters.

At a given incident laser power, the number of photons absorbed by the sensitizer, N_{abs}, is proportional to the emission intensity, I_{em}, divided by the quantum yield of emission, ϕ_{em} (eqn (2)).

$$N_{abs} = \alpha \frac{I_{em}}{\phi_{em}} \qquad (2)$$

The proportionality constant α reflects, among other things, instrumental parameters used in the experiment. The amount of $O_2(a^1\Delta_g)$ formed in a given experiment is likewise proportional to the product of N_{abs} and the $O_2(a^1\Delta_g)$ quantum yield, ϕ_Δ. For our present experiment performed under conditions where α is always the same, the desired equality is shown in eqn (3) where the superscript *ref* refers to the reference compound PpIX.

$$\frac{I_{em}}{\phi_{em}}\phi_\Delta = \frac{I_{em}^{ref}}{\phi_{em}^{ref}}\phi_\Delta^{ref} \qquad (3)$$

In the ideal case, incorporating known values of ϕ_Δ and ϕ_{em} into eqn (3) allows one to ascertain the desired ratio of sensitizer emission intensities, controlled either by the incident laser energy or the sensitizer concentration, that correspond to the same dose of $O_2(a^1\Delta_g)$ from both PpIX and $Ir(ppy)_2(phen)^+$.

Focussing first on $Ir(ppy)_2(phen)^+$, the ϕ_Δ and ϕ_{em} data in Table 1 clearly show the importance of knowing whether this molecule is localized in a hydrophilic or hydrophobic intracellular domain. Moreover, the pertinent parameters depend on the local oxygen concentration and this too will vary with intracellular location (*i.e.*, oxygen is less soluble in water than in typical hydrocarbons). For PpIX, although I_{em} refers to a fluorescent signal that does not appreciably depend on oxygen concentration, the magnitude of ϕ_{em} may depend on intracellular location.[65] Relying on the data in Table 1, a ϕ_Δ(PpIX) value of 0.56 ± 0.03, and a ϕ_{em}^{ref} value of 0.04 for intracellular PpIX,[65] the desired ratio of sensitizer emission intensities, I_{em}/I_{em}^{ref}, that correspond to the same dose of $O_2(a^1\Delta_g)$ from these respective molecules can thus range from ~ 3 for $Ir(ppy)_2(phen)^+$ in a hydrophobic domain to ~ 16 for $Ir(ppy)_2(phen)^+$ in a domain containing H_2O.

To accommodate this domain-dependent uncertainty in the doses of $O_2(a^1\Delta_g)$ delivered upon irradiation of PpIX and $Ir(ppy)_2(phen)^+$, respectively, experiments to assess relative photo-induced cytotoxicity were performed using a range of intracellular concentrations of $Ir(ppy)_2(phen)^+$.

Assessing cell death. Cell responses to irradiation of $Ir(ppy)_2(phen)^+$ and PpIX were assessed using bright field images to record morphology changes associated with cell death (*e.g.*, membrane located vacuole formation, chromatin condensation, cell shrinkage). This is an accepted method that combines reasonable accuracy with ease of implementation.[11, 12, 25, 26, 67-69]

We first established that, in the absence of light, $Ir(ppy)_2(phen)^+$ is not cytotoxic over an observation period of 24 h. These experiments were performed using cells that had been incubated with media containing $Ir(ppy)_2(phen)^+$ over the concentration range of 10^{-7} to 10^{-5} M (see Fig. 3).

For the photo-initiated experiments, the focused irradiation was localized in the mitochondria-rich portion of the cytoplasm. We have previously established that it is advantageous to perform such experiments under conditions where the initial signs of cell death all appear within 180 min after the light dose has been delivered.[12] To this end, we used an average incident laser power of 2.4 mW for cells incubated in H_2O-based media. The two-photon irradiation exposure period was 30 min (80 MHz laser). We then counted the number of cells that showed a given morphological feature of death 150 min after the end of actinic irradiation. Representative data are shown in Fig. 8.

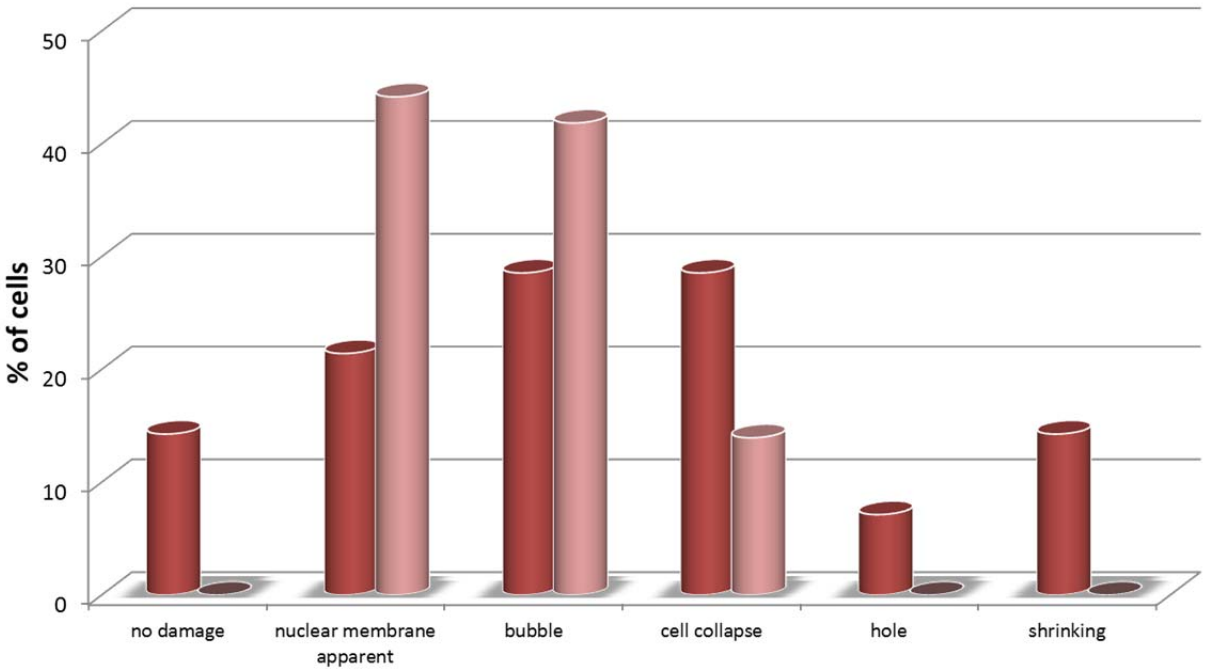

Figure 8. Histogram comparing different morphological features associated with cell death for data recorded upon irradiation of 14 cells containing $Ir(ppy)_2(phen)^+$ (dark pylons) and, independently, 18 cells containing PpIX (lighter pylons). In many cases, a given cell would show more than one morphological sign of death. These data were recorded using cells incubated in a medium containing 0.35 μM $Ir(ppy)_2(phen)^+$ (see Fig. 3) and correspond to a I_{em}/I_{em}^{ref} ratio of 3.5 (*i.e.*, $Ir(ppy)_2(phen)^+$ in a hydrophobic intracellular domain, see text). The differences between the PpIX and $Ir(ppy)_2(phen)^+$ data for a given morphological response have no statistical significance indicating that $O_2(a^1\Delta_g)$ sensitized by these respective dyes is equally cytotoxic under these conditions (non-directional *z* hypothesis test[12]).

The data in Fig. 8 were recorded under conditions that yield $I_{em}/I_{em}^{ref} = 3.5$. Recall that this ratio characterizes a situation where PpIX and $Ir(ppy)_2(phen)^+$ would deliver the same dose of $O_2(a^1\Delta_g)$, with the stipulation that $Ir(ppy)_2(phen)^+$ is principally localized in a hydrophobic domain. Given the log $P_{o/w} = 1.67$ value for $Ir(ppy)_2(phen)^+$ and the spectrum in Fig. 6, we believe this is a reasonably accurate condition to assess the cytotoxicity of $Ir(ppy)_2(phen)^+$. The data obtained clearly show that, under these conditions, $Ir(ppy)_2(phen)^+$ and PpIX are equally cytotoxic. Thus, our initial observation that $Ir(ppy)_2(phen)^+$-containing cells are quite sensitive to room lighting,

certainly in comparison to cells containing PpIX or other porphyrin-based sensitizers, appears to be a consequence of the fact that a high intracellular concentration of $Ir(ppy)_2(phen)^+$ is rapidly achieved upon incubation in a medium containing $Ir(ppy)_2(phen)^+$.

On the other hand, if, for some reason, a non-negligible amount of intracellular $Ir(ppy)_2(phen)^+$ is principally localized in a more hydrophilic domain, then the data in Fig. 8 would indicate that the $O_2(a^1\Delta_g)$ produced by $Ir(ppy)_2(phen)^+$ is appreciably more cytotoxic than the $O_2(a^1\Delta_g)$ produced by PpIX. This point was confirmed by monitoring cell death under conditions where $I_{em}/I_{em}^{ref} = 16$, and irradiation of $Ir(ppy)_2(phen)^+$ was indeed appreciably more cytotoxic than irradiation of PpIX. To reiterate, however, we believe that the data in Fig. 6 confirm that $Ir(ppy)_2(phen)^+$ is principally localized in hydrophobic intracellular domains and the appropriate condition to monitor the relative cytotoxicity of $Ir(ppy)_2(phen)^+$ and PpIX is $I_{em}/I_{em}^{ref} = 3.5$. The pertinent data are thus shown in the histogram of Fig. 8.

Because both $Ir(ppy)_2(phen)^+$ and PpIX appear to be localized in the same organelle (the mitochondria) and because the diffusion distance of intracellular $O_2(a^1\Delta_g)$ is sufficiently large relative to the size of a mitochondrion,[2] it seems unlikely that the $O_2(a^1\Delta_g)$ produced by $Ir(ppy)_2(phen)^+$ would be more cytotoxic than $O_2(a^1\Delta_g)$ produced by PpIX as a consequence of targeting different location-dependent intracellular receptors (*e.g.*, proteins). This point is again consistent with the data in Fig. 8.

$O_2(a^1\Delta_g)$ *is the cytotoxic agent.* With the preceding discussion in mind, it is important to establish that $O_2(a^1\Delta_g)$ is indeed the initial photo-produced reactive intermediate responsible for adverse cell response in these studies. To this end, we first found that irradiation of $Ir(ppy)_2(phen)^+$ in cells that had been incubated in a D_2O-based medium showed morphological signs of death much sooner than cells incubated in an H_2O-based medium. This is consistent with the fact that the lifetime of

$O_2(a^1\Delta_g)$ is appreciably longer in D_2O than in H_2O and hence, in D_2O-incubated cells, (1) the intracellular diffusion distance of $O_2(a^1\Delta_g)$ is greater, and (2) the probability for reaction of $O_2(a^1\Delta_g)$ with a given substrate is likewise greater.[2] Other cytotoxic ROS that might be initially produced (*e.g.*, the superoxide ion) do not have a corresponding response to changes in the solvent H/D isotopic composition. Second, upon the addition of an efficient and specific $O_2(a^1\Delta_g)$ quencher to the D_2O-based medium (*i.e.*, 10 mM NaN_3), we were unable to initiate cell death upon irradiation of either PpIX or $Ir(ppy)_2(phen)^+$. We independently established using time-resolved absorption experiments that NaN_3 does not quench the triplet states of both $Ir(ppy)_2(phen)^+$ and PpIX. Thus, the protective effect exerted by NaN_3 is indeed a consequence of quenching $O_2(a^1\Delta_g)$, not the precursor to $O_2(a^1\Delta_g)$. [Although NaN_3 is itself cytotoxic over long time periods, it is benign over the time periods of our studies.[67, 70]]

Conclusion

We have identified a cyclometallated Ir(III) complex whose ability to photosensitize the production of $O_2(a^1\Delta_g)$ depends strongly on the local environment of this molecule. This sensitivity to the local environment points to a problem that could influence many $O_2(a^1\Delta_g)$ photosensitized experiments in cells. Specifically, the control and quantification of the $O_2(a^1\Delta_g)$ "dose" can be difficult which, in turn, can be a hindrance in mechanistic studies of $O_2(a^1\Delta_g)$ behavior. The data reported herein provide a nice justification for the design and development, for example, of genetically-encoded protein-encapsulated sensitizers.[19, 71] In the ideal case under these latter conditions, the local environment of the sensitizer will remain the same and photophysical data recorded from a bulk *in vitro* solution would be valid for an application *in vivo*. The data reported herein likewise provide a nice justification for experiments in which intracellular $O_2(a^1\Delta_g)$ is selectively produced upon the irradiation of oxygen itself in sensitizer-free experiments.[72]

Acknowledgements

This work was supported by the Danish National Research Foundation. S. T. thanks the Japan Society for the Promotion of Science institutional program for young researcher's overseas visits.

References

1 E. L. Clennan and A. Pace, Advances in Singlet Oxygen Chemistry, *Tetrahedron*, 2005, **61**, 6665-6691.

2 P. R. Ogilby, Singlet Oxygen: There is Indeed Something New Under the Sun., *Chem. Soc. Rev.*, 2010, **39**, 3181-3209.

3 L.-O. Klotz, K.-D. Kröncke and H. Sies, Singlet Oxygen-Induced Signaling Effects in Mammalian Cells, *Photochem. Photobiol. Sci.*, 2003, **2**, 88-94.

4 R. Bonnett, *Chemical Aspects of Photodynamic Therapy*, Gordon and Breach Science Publishers, Amsterdam, 2000.

5 R. W. Redmond and I. E. Kochevar, Spatially-Resolved Cellular Responses to Singlet Oxygen, *Photochem. Photobiol.*, 2006, **82**, 1178-1186.

6 D. Phillips, Light relief: photochemistry and medicine, *Photochem. Photobiol. Sci.*, 2010, **9**, 1589-1596.

7 A. Blázquez-Castro, T. Breitenbach and P. R. Ogilby, Singlet oxygen and ROS in a new light: low-dose subcellular photodynamic treatment enhances proliferation at the single cell level., *Photochem. Photobiol. Sci.*, 2014, **13**, 1235-1240.

8 C. Schweitzer and R. Schmidt, Physical Mechanisms of Generation and Deactivation of Singlet Oxygen, *Chem. Rev.*, 2003, **103**, 1685-1757.

9 N. Rubio, S. P. Fleury and R. W. Redmond, Spatial and Temporal Dynamics of *in vitro* Photodynamic Cell Killing: Extracellular Hydrogen Peroxide Mediates Neighboring Cell Death., *Photochem. Photobiol. Sci.*, 2009, **8**, 457-464.

10 T. Breitenbach, P. R. Ogilby and J. D. C. Lambert, Effect of Intracellular Photosensitized Singlet Oxygen Production on the Electrophysiological Properties of Cultured Rat Hippocampal Neurons., *Photochem. Photobiol. Sci.*, 2010, **9**, 1621-1633.

11 F. M. Pimenta, R. L. Jensen, L. Holmegaard, T. V. Esipova, M. Westberg, T. Breitenbach and P. R. Ogilby, Singlet-Oxygen-Mediated Cell Death Using Spatially-Localized Two-Photon Excitation of an Extracellular Sensitizer, *J. Phys. Chem. B*, 2012, **116**, 10234-10246.

12 A. Gollmer, F. Besostri, T. Breitenbach and P. R. Ogilby, Spatially resolved two-photon irradiation of an intracellular singlet oxygen photosensitizer: Correlating cell response to the site of localized irradiation., *Free Rad. Res.*, 2013, **47**, 718-730.

13 R. Schmidt, C. Tanielian, R. Dunsbach and C. Wolff, Phenalenone, a Universal Reference Compound for the Determination of Quantum Yields of Singlet Oxygen Sensitization, *J. Photochem. Photobiol., A: Chem.*, 1994, **79**, 11-17.

14 E. Oliveros, P. Suardi-Murasecco, T. Aminian-Saghafi and A. M. Braun, 1H-Phenalen-1-one: Photophysical Properties and Singlet Oxygen Production., *Helv. Chim. Acta*, 1991, **74**, 79-90.

15 C. Marti, O. Jürgens, O. Cuenca, M. Casals and S. Nonell, Aromatic Ketones as Standards for Singlet Molecular Oxygen $O_2(^1\Delta_g)$ Photosensitization. Time-Resolved Photoacoustic and Near-IR Emission Studies., *J. Photochem. Photobiol., A. Chem.*, 1996, **97**, 11-18.

16 F. Wilkinson, W. P. Helman and A. B. Ross, Quantum Yields for the Photosensitized Formation of the Lowest Electronically Excited Singlet State of Molecular Oxygen in Solution, *J. Phys. Chem. Ref. Data*, 1993, **22**, 113-262.

17 P.-G. Jensen, J. Arnbjerg, L. P. Tolbod, R. Toftegaard and P. R. Ogilby, Influence of an Intermolecular Charge-Transfer State on Excited-State Relaxation Dynamics: Solvent Effect on the Methylnaphthalene-Oxygen System and its Significance for Singlet Oxygen Production., *J. Phys. Chem. A*, 2009, **113**, 9965-9973.

18 E. Alarcon, A. M. Edwards, A. Aspee, F. E. Moran, C. D. Borsarelli, E. A. Lissi, D. Gonzalez-Nilo, H. Poblete and J. C. Scaiano, Photophysics and photochemistry of dyes bound to human serum albumin are determined by the dye localization, *Photochem. Photobiol. Sci.*, 2010, **9**, 93-102.

19 M. Westberg, L. Holmegaard, F. M. Pimenta, M. Etzerodt and P. R. Ogilby, Rational Design of an Efficient, Genetically Encodable, Protein-Encased Singlet Oxygen Photosensitizer, *J. Am. Chem. Soc.*, 2015, **137**, 1632-1642.

20 J. Arnbjerg, M. Johnsen, P. K. Frederiksen, S. E. Braslavsky and P. R. Ogilby, Two-Photon Photosensitized Production of Singlet Oxygen: Optical and Optoacoustic Characterization of Absolute Two-Photon Absorption Cross Sections for Standard Sensitizers in Different Solvents., *J. Phys. Chem. A*, 2006, **110**, 7375-7385.

21 J. Arnbjerg, M. J. Paterson, C. B. Nielsen, M. Jørgensen, O. Christiansen and P. R. Ogilby, One- and Two-Photon Photosensitized Singlet Oxygen Production: Characterization of Aromatic Ketones as Sensitizer Standards., *J. Phys. Chem. A*, 2007, **111**, 5756-5767.

22 C. B. Nielsen, J. Arnbjerg, M. Johnsen, M. Jørgensen and P. R. Ogilby, Molecular Tuning of Phenylene-Vinylene Derivatives for Two-Photon Photosensitized Singlet Oxygen Production, *J. Org. Chem.*, 2009, **74**, 9094-9104.

23 M. Johnsen and P. R. Ogilby, Effect of Solvent on Two-Photon Absorption by Vinyl Benzene Derivatives, *J. Phys. Chem. A.*, 2008, **112**, 7831-7839.

24 D. Hrsak, L. Holmegaard, A. S. Poulsen, N. H. List, J. Kongsted, M. P. Denofrio, R. Erra-Balsells, F. M. Cabrerizo, O. Christiansen and P. R. Ogilby, Experimental and computational study of solvent effects on one- and two-photon absorption spectra of chlorinated harmines., *Phys. Chem. Chem. Phys.*, 2015, **17**, 12090-12099.

25 B. W. Pedersen, T. Breitenbach, R. W. Redmond and P. R. Ogilby, Two-photon irradiation of an intracellular singlet oxygen photosensitizer: achieving localized subcellular excitation in spatially-resolved experiments *Free Rad. Res.*, 2010, **44**, 1383-1397

26 T. Breitenbach, M. K. Kuimova, P. Gbur, S. Hatz, N. B. Schack, B. W. Pedersen, J. D. C. Lambert, L. Poulsen and P. R. Ogilby, Photosensitized Production of Singlet Oxygen: Spatially-Resolved Optical Studies in Single Cells., *Photochem. Photobiol. Sci.*, 2009, **8**, 442-452.

27 J. N. Demas and G. A. Crosby, The Measurement of Photoluminescence Quantum Yields. A Review., *J. Phys. Chem.*, 1971, **75**, 991-1024.

28 R. D. Scurlock, S. Nonell, S. E. Braslavsky and P. R. Ogilby, Effect of Solvent on the Radiative Decay of Singlet Molecular Oxygen ($a^1\Delta_g$), *J. Phys. Chem.*, 1995, **99**, 3521-3526.

29 N. S. Makarov, M. Drobizhev and A. Rebane, Two-photon absorption standards in the 550-1600 nm excitation wavelength range, *Optics Express*, 2008, **16**, 4029-4047.

30 W.-C. Sun, K. R. Gee, D. H. Klaubert and R. P. Haugland, Synthesis of Fluorinated Fluoresceins, *J. Org. Chem.*, 1997, **62**, 6469-6475.

31 E. Skovsen, J. W. Snyder and P. R. Ogilby, Two-photon singlet oxygen microscopy: the challenges of working with single cells., *Photochem. Photobiol.*, 2006, **82**, 1187-1197.

32 R. V. Kiran, C. F. Hogan, B. D. James and D. J. D. Wilson, Photophysical and Electrochemical Properties of Phenanthroline-Based Bis-cyclometallated Iridium Complexes in Aqueous and Organic Media, *Eur. J. Inorg. Chem.*, 2011, 4816-4825.

33 S. Nonell, M. Gonzalez and F. R. Trull, 1H-Phenalen-1-one-2-sulfonic acid: An Extremely Efficient Singlet Molecular Oxygen Sensitizer for Aqueous Media., *Afinidad*, 1993, **448**, 445-450.

34 S. Hatz, J. D. C. Lambert and P. R. Ogilby, Measuring the Lifetime of Singlet Oxygen in a Single Cell: Addressing the Issue of Cell Viability, *Photochem. Photobiol. Sci.*, 2007, **6**, 1106-1116.

35 M. P. Denofrio, C. Lorente, T. Breitenbach, S. Hatz, F. M. Cabrerizo, A. H. Thomas and P. R. Ogilby, Photodynamic Effects of Pterin on HeLa Cells., *Photochem. Photobiol.*, 2011, **87**, 862-866.

36 P. Suppan and N. Ghoneim, *Solvatochromism*, The Royal Society of Chemistry, Cambridge, 1997.

37 J. Li, P. I. Djurovich, B. D. Alleyne, M. Yousufuddin, N. N. Ho, J. C. Thomas, J. C. Peters, R. Bau and M. E. Thompsen, Synthetic Control of Excited-State Properties in Cyclometalated Ir(III) Complexes Using Ancillary Ligands., *Inorg. Chem.*, 2005, **44**, 1713-1727.

38 J. Van Houten and R. J. Watts, The Effect of Ligand and Solvent Deuteration on the Excited State Properties of the Tris(2,2'-bipyridyl)ruthenium(II) Ion in Aqueous Solution. Evidence for Electron Transfer to Solvent., *J. Am. Chem. Soc.*, 1975, **97**, 3843-3844.

39 R. Sriram and M. Z. Hoffman, Solvent Isotope Effect on the Photophysics of $Ru(bpy)_3^{2+}$ and $Ru(phen)_3^{2+}$ in Aqueous Solution at Room Temperature, *Chem. Phys. Lett.*, 1982, **85**, 572-575.

40 W. R. Cherry and L. J. Henderson, Relaxation Processes of Electronically Excited States in Polypyridine Ruthenium Complexes, *Inorg. Chem.*, 1984, **23**, 983-986.

41 A. Masuda and Y. Kaizu, Specific Role of Water in Radiationless Transition from the Triplet MLCT States of Tris(polypyridine) Complexes of Osmium(II), *Inorg. Chem.*, 1998, **37**, 3371-3375.

42 A. A. Abdel-Shafi, M. D. Ward and R. Schmidt, Mechanism of quenching by oxygen of the excited states of ruthenium(II) complexes in aqueous media. Solvent isotope effect and photosensitized generation of singlet oxygen, $O_2(^1\Delta_g)$, by $[Ru(diimine)(CN)_4]^{2-}$ complex ions, *Dalton Trans.*, 2007, 2517-2527.

43 F. Wilkinson, W. P. Helman and A. B. Ross, Rate Constants for the Decay and Reactions of the Lowest Electronically Excited Singlet State of Molecular Oxygen in Solution. An Expanded and Revised Compilation., *J. Phys. Chem. Ref. Data*, 1995, **24**, 663-1021.

44 S. Takizawa, R. Aboshi and S. Murata, Photooxidation of 1,5-dihydroxynaphthalene with iridium complexes as singlet oxygen sensitizers., *Photochem. Photobiol. Sci.*, 2011, **10**, 895-903.

45 P. I. Djurovich, D. Murphy, M. E. Thompsen, B. Hernandez, R. Gao, P. L. Hunt and M. Selke, Cyclometalated iridium and platinum complexes as singlert oxygen photosensitizers: quantum yields, quenching rates and correlation with electronic structures., *Dalton Trans.*, 2007, 3763-3770.

46 L. Flamigni, A. Barbieri, C. Sabatini, B. Ventura and F. Barigelletti, Photochemistry and Photophysics of Coordination Compounds: Iridium, *Top. Curr. Chem.*, 2007, **281**, 143-203.

47 Y. You and W. Nam, Photofunctional triplet excited states of cyclometalated Ir(III) complexes: beyond electroluminescence., *Chem. Soc. Rev.*, 2012, **41**, 7061-7084.

48 R. Gao, D. G. Ho, B. Hernandez, M. Selke, D. Murphy, P. I. Djurovich and M. E. Thompsen, Bis-cyclometalated Ir(III) Complexes as Efficient Singlet Oxygen Sensitizers, *J. Am. Chem. Soc.*, 2002, **124**, 14828-14829.

49 S. P.-Y. Li, C. T.-S. Lau, M.-W. Louie, Y.-W. Lam, S.-H. Cheng and K. K.-W. Lo, Mitochondria-targeting cyclometalated iridium(III)-PEG complexes with tunable photodynamic activity, *Biomaterials*, 2013, **34**, 7519-7532.

50 D. Ashen-Garry and M. Selke, Singlet Oxygen Generation by Cyclometalated Complexes and Applications, *Photochem. Photobiol.*, 2014, **90**, 257-274.

51 A. A. Abdel-Shafi, D. R. Worrall and A. Y. Ershov, Photosensitized generation of singlet oxygen from ruthenium(II) and osmium(II) bipyridyl complexes., *Dalton Trans.*, 2004, 30-36.

52 D. Garcia-Fresnadillo, Y. Georgiadou, G. Orellana, A. M. Braun and E. Oliveros, Singlet Oxygen Production by Ruthenium(II) Complexes Containing Polyazaheterocyclic Ligands in Methanol and Water, *Helv. Chim. Acta*, 1996, **79**, 1222-1238.

53 R. M. Edkins, S. L. Bettington, A. E. Goeta and A. Beeby, Two-photon spectroscopy of cyclometalated iridium complexes., *Dalton Trans.*, 2011, **40**, 12765-12770.

54 L. S. Natrajan, A. Toulmin, A. Chew and S. W. Magennis, Two-photon luminescence from polar bis-terpyridyl-stilbene derivatives of Ir(III) and Ru(II), *Dalton Trans.*, 2010, **39**, 10837-10846.

55 M. Pawlicki, H. A. Collins, R. G. Denning and H. L. Anderson, Two-Photon Absorption and the Design of Two-Photon Dyes, *Angew. Chem. Int. Ed.*, 2009, **48**, 3244-3266.

56 R. Cao, J. Jia, X. Ma, M. Zhou and H. Fei, Membrane Localized Iridium(III) Complex Induces Endoplasmic Reticulum Stress and Mitochondria-Mediated Apoptosis in Human Cancer Cells, *J. Med. Chem.*, 2013, **56**, 3636-3644.

57 K. K.-W. Lo and K. Y. Zhang, Iridium(III) complexes as therapeutic and bioimaging reagents for cellular applications., *RSC Adv.*, 2012, **2**, 12069-12083.

58 R. P. Haugland, *Handbook of Fluorescent Probes and Research Products*, Molecular Probes, Inc., Eugene, OR, 2002.

59 B. Alberts, A. Johnson, J. Lewis, M. Raff, K. Roberts and P. Walter, *Molecular Biology of the Cell*, Garland Science, New York, 2002.

60 L. V. Johnson, M. L. Walsh and L. B. Chen, Localization of Mitochondria in Living Cells with Rhodamine 123, *Proc. Natl. Acad. Sci. USA*, 1980, **77**, 990-994.

61 D. Kessel, Correlation between subcellular localization and photodynamic therapy, *J. Porphyrins Phthalocyanines*, 2004, **8**, 1009-1014.

62 E. F. Gudgin Dickson, J. C. Kennedy and R. H. Pottier, *Photodynamic Therapy using 5-Aminolevulinic Acid-Induced Protoporphyrin IX* in *Photodynamic Therapy*, ed. T. Patrice, Royal Society of Chemistry, Cambridge, 2003, pp. 81-103

63 J. M. Fernandez, M. D. Bilgin and L. I. Grossweiner, Singlet oxygen generation by photodynamic agents, *J. Photochem. Photobiol. B: Biol.*, 1997, **37**, 131-140.

64 R. W. Redmond and J. N. Gamlin, A compilation of singlet oxygen yields from biologically relevant molecules, *Photochem. Photobiol.*, 1999, **70**, 391-475.

65 G. I. Lozovaya, Z. Masinovsky and A. A. Sivash, Protoporphyrin IX as a Possible Ancient Photosensitizer: Spectral and Photochemical Studies, *Origins of Life and Evolution of Biospheres*, 1990, **20**, 321-330.

66 J. Squier and M. Müller, High resolution nonlinear microscopy: A review of sources and methods for achieving optimal imaging, *Rev. Sci. Instrum.*, 2001, **72**, 2855-2867.

67 B. W. Pedersen, L. E. Sinks, T. Breitenbach, N. B. Schack, S. A. Vinogradov and P. R. Ogilby, Single Cell Responses to Spatially-Controlled Photosensitized Production of Extracellular Singlet Oxygen, *Photochem. Photobiol.*, 2011, **87**, 1077-1091.

68 G. Häcker, The morphology of apoptosis, *Cell Tissue Res.*, 2000, **301**, 5-17.

69 S. Rello, J. C. Stockert, V. Moreno, A. Gámez, M. Pacheco, A. Juarranz, M. Cañete and A. Villanueva, Morphological criteria to distinguish cell death induced by apoptotic and necrotic treatments., *Apoptosis*, 2005, **10**, 201-208.

70 M. K. Kuimova, G. Yahioglu and P. R. Ogilby, Singlet Oxygen in a Cell: Spatially Dependent Lifetimes and Quenching Rate Constants, *J. Am. Chem. Soc.*, 2009, **131**, 332-340.

71 J. Torra, A. Burgos-Caminal, S. Endres, M. Wingen, T. Drepper, T. Gensch, R. Ruiz-González and S. Nonell, Singlet oxygen photosensitization by the fluoprescent protein Pp2FbFP L30M, a novel derivative of *Pseudomonas putida* flavin-binding Pp2FbFP, *Photochem. Photobiol. Sci.*, 2015, **14**, 280-287.

72 M. Bregnhøj, A. Blázquez-Castro, M. Westberg, T. Breitenbach and P. R. Ogilby, Direct 765 nm Optical Exciation of Molecular Oxygen in Solution and in Single Mammalian Cells, *J. Phys. Chem. B*, 2015, **119**, 5422-5429.

Table of Contents Graphic: